TEORIJSKA I PRIMENJENA MEHANIKA 15, pp 7–18, 1989, UDK 534

CHAOTIC MOTION OF ROTOR

L. Cvetićanin

(Received 19.09.1989; Revised 29.12.1989)

1. Introduction. Rotors are the fundamental working elements of a lot of machines. The rotors are usually made of metalic materials, but some of them are made of non-metalic materials. The properties of these materials are non-linear. For these rotors it is evident that the characteristics of motion depends on the value of the parameters. Two types of rotation are the most usual:

1. the trajectory of rotor's center is a circle around the start postition of the rotor's axle (large orbit) (Fig. 1.a.)

2. there is a deflection of rotor's center and the rotor rotates around this position (small orbit) (Fig. 1.b).

(In Fig.1. S_0 is the start position of rotor's center and S_0xys is a fixed coordinate system.)

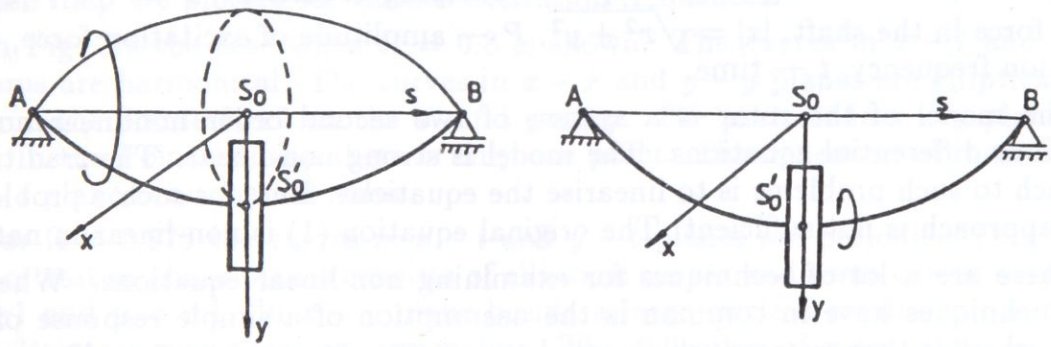

Fig. 1. The trajectories of rotor's center

But, for some parameters of rotor the motion is quite unusual, and it differs from motion in Fig. 1a and 1b. Then, the efficiency and the productivity of machines are smaller. The operator have to vary the working parameters of the rotor till the phenomena dissapear. Nowadays, there are a lot of papers which are dealing with various kinds of motion of the mechanical systems. In the papers [1–6] the chaotic motion of the one-degree-freedom systems described by Duffing equations with soft, rigid and zero elastic characteristics are analysed. The physical sence of

chaos is given in papers [7–12] for these systems. In this paper various kinds of rotor's motion are analysed, the parameters which have an influence on the motion are denoted and the criteries for obtaining parameters for some motions of center are defined.

2. Model of Rotor. Rotor which is analysed is a shaft-disc system (Fig.2).

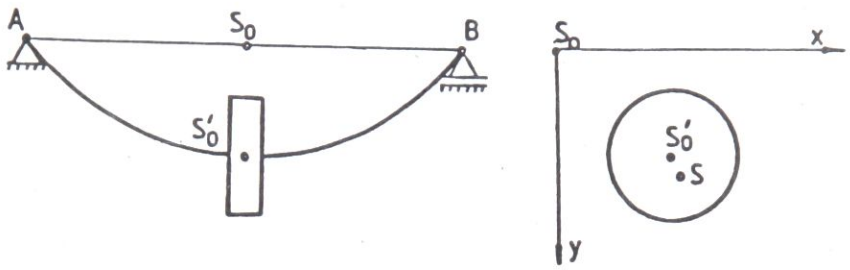

Fig. 2. Model of rotor

It is a shaft-disc system. The disc is symmetrically settled in the middle of the shaft. The mass of the shaft is neglictible in comparation to the mass of the disc. The shaft is supported in two bearings. The shaft has a circular cross section. The mathematical model is after the paper [13]

$$\ddot{z} + h\dot{z} + zF(|z|) = Pe^{i\Omega t} \tag{1}$$

where: $z = x + iy$ is the complex deflection function, x, y — deflection in x, y direction of fixed coordinate system S_0xys settled in the start postition of rotor's center, $i = \sqrt{-1}$ — imaginary unit, h — damping coefficient, $F = -1 + |z|^2$ — elastic force in the shaft, $|z| = \sqrt{x^2 + y^2}$, P — amplitude of excitation force, Ω — excitation frequency, t — time.

The model of the rotor is a system of two second order nonlinear nonhomogenious differential equations. The model is strong non-linear. The traditional approach to such problems is to linearise the equations. But, for such a problem a linear approach is not sufficient. The original equation (1) is non-linear in nature.

There are a lot of techniques for examining non-linear equations. What all these techniques have in common is the aasumption of a simple response of the system which is then successively iterated upon to convergate to a "good" approximation to the actual response. Some motions are beyond the scope of approximate analytical method and the technique is completely unable to capture the essentials of resulting motion.

The analyses of eq. (1) is done numerically. The differential equations are solved by Runge-Kutta method.

3. Descriptors of Motion. To observe the motion and to better understand it, several descriptors are available. Among these are: Poincare map and phase plane portraits [1,2,4,10], power spectral density [3], stochastic sensitivity function [14], probability density function [15–16], Lyapunov's exponent [17], autocorrelation function [5], time history [7,8]. It can be concluded that only one descriptor is not enough to analyse the motion. Some of them had to be used together.

In the paper the motion of the rotor described by (1) is observed by portraits in $x-\dot{x}$, $y-\dot{y}$, $z-\dot{z}$ planes, Poincare map and time history diagrams. These descriptors can be denoted numerically. For the correct numerical description the time step had to be defined. It is well known that there exists a difference between exact analytical solutions of differential equations and numerical integrations of the equations. The analytical solutions are continuous in time and numerical integrations involve finite time steps. Because of this, numerical integrations are best regarded as the solutions of difference equations rather than differential equations. For small time steps the difference between differential and difference equation is presumed to vanish [6]. To denote the time step is not an easy task. The improper choise of time step can cause spurious results. It is the question which integration method depends less of the time step. In the paper [18] two explicit and four implicit numerical integration methods for ordinary second order nonlinear differential equations are compared. The Runge-Kutta and central difference methods are the most efficient, they do not require small time steps to achive low error. Because of that Runge-Kutta method is applied in this paper.

In accordance with the paper [6] the parameters of influence on the cahracter of motion are: the initial values, $x(0)$, $y(0)$, $\dot{x}(0)$ and $\dot{y}(0)$, excitation frequency Ω and the excitation amplitude P. In the paper only the excitation frequency is varied.

4. Observation of the Motion. The numerical values of rotor's parameters are: damping coefficient $h = 0.2$ and excitation amplitude $P = 0.25$, and the initial conditions $x(0) = y(0) = -0.2$, $\dot{x}(0) = \dot{y}(0) = 0$. The excitation frequency in varied in the interval $\Omega = 0.5$–2.

In Fig. 3. the solutions of eq. (1) in $x-\dot{x}$, $y-\dot{y}$, $x-y$, $x-t$, $A-t$ planes and Poincare map are plotted for various excitation frequences.

In Fig. 3.a the case when $\Omega = 0.8$ is shown. The curves in $x-t$ and $y-t$ diagrams are harmonical. The curves in $x-\dot{x}$ and $y-\dot{y}$ planes are elliptical and surround the points $0, \pm 1$ on the x- and y-axles. The portrait in $x-y$ plane is a circle. In the Poincare map there is only one point. The deflection of mass center in $A-t$ plane is a constant value.

For $\Omega = 0.975$ the curves in $x-t$ and $y-t$ planes are periodical (Fig. 3.b). The portrait in phase planes consists of elliptical curves and some curves surround $x = \pm 1$ and $y = \pm 1$. In $x-y$ plane beside a large circle a small orbit appears. In the Poincare map there are two points. The deflection of mass center in $A-t$ plane is a double-periodical function.

By increasing of excitation frequency to $\Omega = 0.99$ the curves in phase planes are more complex. The curve irregular deflects from a closed curve aroung $+1$ to -1 and around 0 (Fig. 3.c). The curves in $x-t$ and $y-t$ planes are non-periodical. In Poincare map the strange attractor is plotted. The trajectory in $x-y$ plane is after a long period of time a system of a large orbit and a lot of irregular settled small orbits which form a black ring. The $A-t$ diagram is non-periodical.

In the Fig. 3.d for $\Omega = 1.2$ the portrait in $x-y$ plane is a small circular orbit. The $A-t$ diagram is a harmonic function of small amplitude. The portrait in Poincare map is only one point. In the phase planes ellipses surround $x = -1$ and $y = -1$.

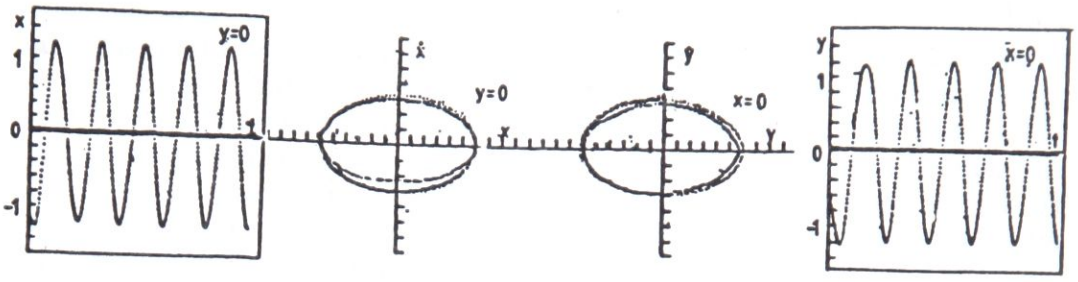
x
1
0
-1
y=0
t
x
y=0
y
x=0
y
1
0
-1
x=0
t

a.

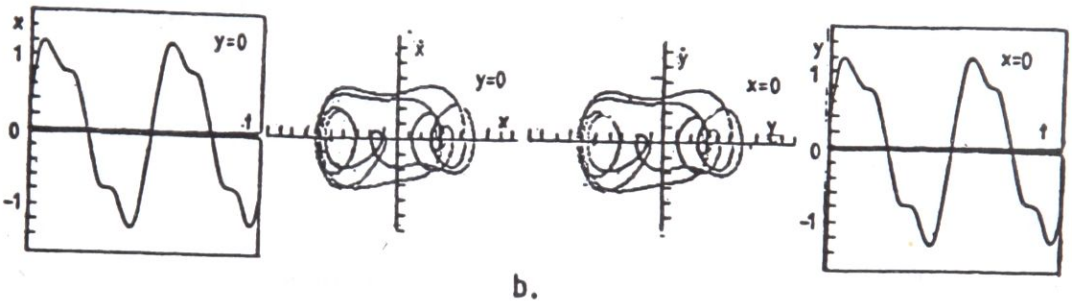
x
1
0
-1
y=0
t
x
y=0
y
x=0
y
1
0
-1
x=0
t

b.

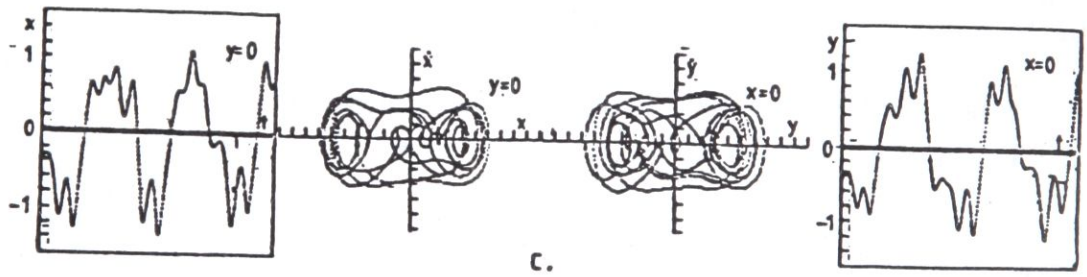
x
1
0
-1
y=0
t
x
y=0
y
x=0
y
1
0
-1
x=0
t

c.

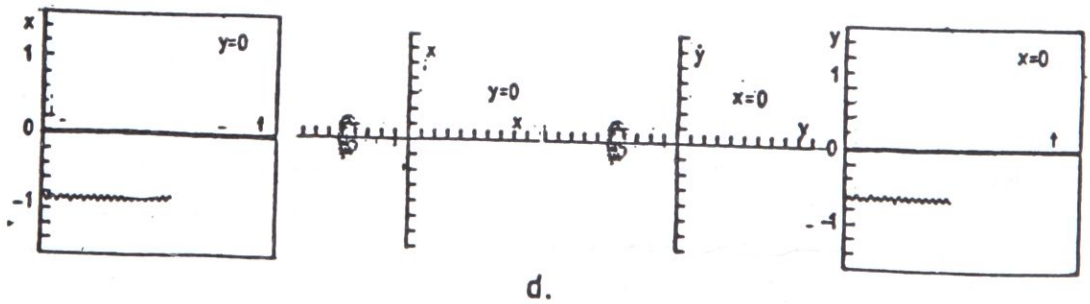
x
1
0
-1
y=0
t
x
y=0
y
x=0
y
1
0
-1
x=0
t

d.

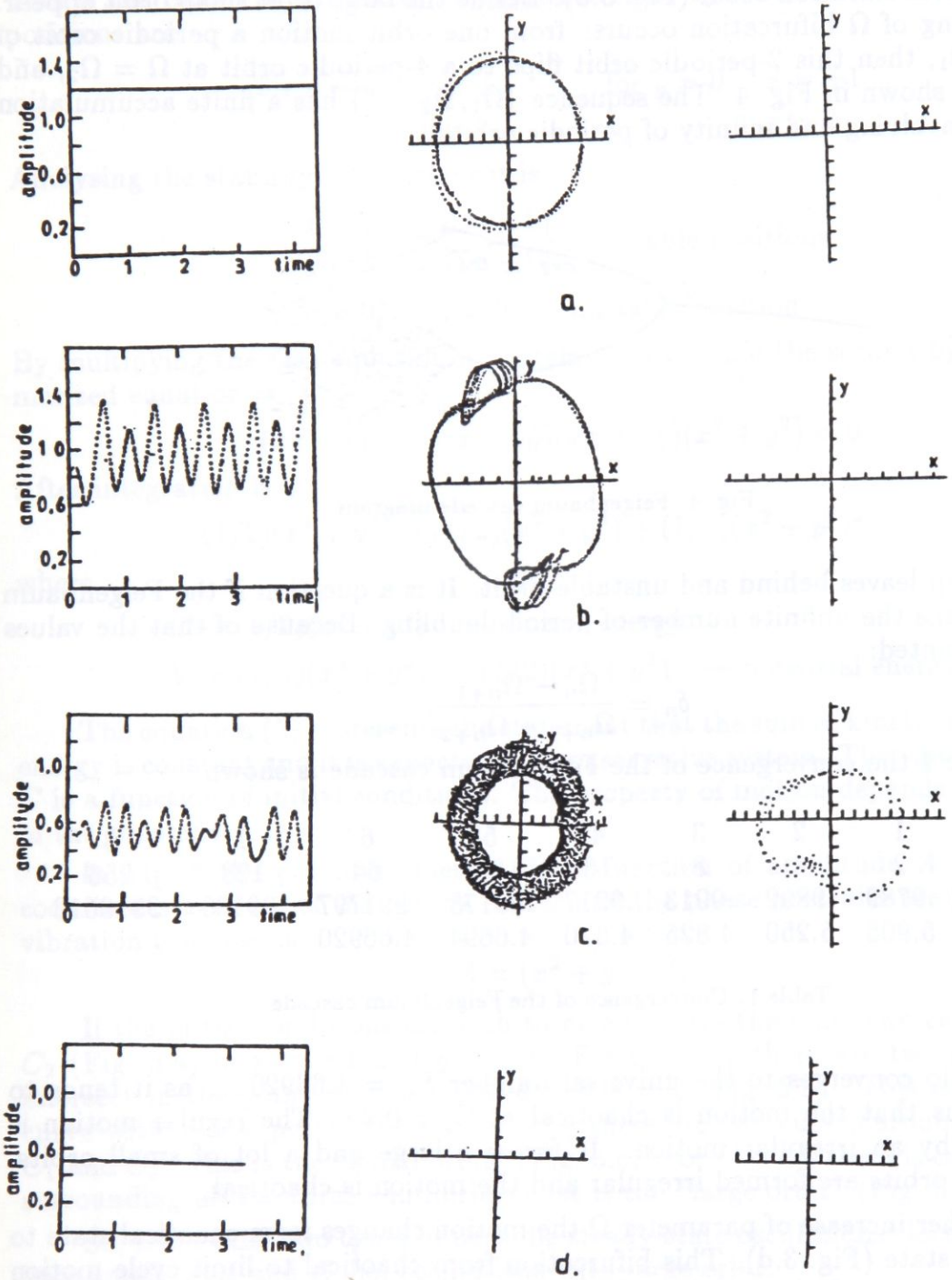

Fig. 3. Descriptors in $x-t$, $x-\dot{x}$, $y-\dot{y}$, $y-t$, $A-t$, $x-y$ planes and Poincare map for: a) $\Omega = 0.8$, b) $\Omega = 0.975$, c) $\Omega = 0.99$, d) $\Omega = 1.2$.

5. Discussion. The varying of excitation parameters causes varying of the property of rotor's center motion. For the small values of excitation parameter the motion is harmonical (Fig. 3.a). For higher values of excitation parameter subharmonical vibration occur (Fig. 3.b). Beside the large orbit small orbit appear. By increasing of Ω bifurcation occurs: from one orbit motion a periodic orbit of 2 at $\Omega = \Omega_1$, then this 2-periodic orbit flips to a 4-periodic orbit at $\Omega = \Omega_2$, and so on, as is shown in Fig. 4. The sequence $\{\Omega_1, \Omega_2, \dots\}$ has a finite accumulation point Ω_∞ involving and infinity of periodic orbits.

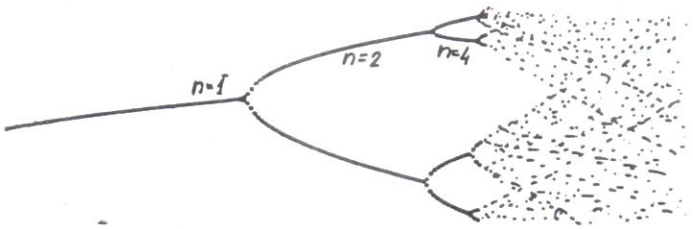

Fig. 4. Feigenbaum cascade diagram

Each flip leaves behind and unstable orbit. It is a question if the Feigenbaum cascade means the unfinite number of period doubling. Because of that the values of δ_n are counted:

$$\delta_n = \frac{\Omega_n - \Omega_{n+1}}{\Omega_{n+1} - \Omega_{n+2}}.$$

In the Table 1 the convergence of the Feigenbaum cascade is shown.

n	0	1	2	3	4	5	6	7	8
period	1	2	4	8	16	32	64	128	256
Ω_n		.9789	.9892	.9913	.9917	.99178	.991797	.99180	.9918013
δ_n		5.905	5.250	4.825	4.670	4.6694	4.66920		

Table 1: Convergence of the Feigenbaum cascade

The ratio converges to the universal number $\delta_\infty = 4.66920\dots$ as it tends to ∞. It means that the motion is chaotical at $\Omega = 0.99$. The regular motion is substituted by an irregular motion. It forms a large and a lot of small orbits. These small orbits are formed irregular and the motion is chaotical.

By further increase of parameter Ω the motion changes form chaotical state to a periodical state (Fig. 3.d). This bifurcation from chaotical to limit cycle motion is intermittency explosion. The rotor's center deflects and rotates around this position. The motion is harmonical.

6. Explanation of Existence of Chaos. The system of differential equations (1) is

$$\begin{aligned} \ddot{x} + h\dot{x} - x + x(x^2 + y^2) &= P\cos\Omega t \\ \ddot{y} + h\dot{y} - y + y(x^2 + y^2) &= P\sin\Omega t. \end{aligned} \tag{2}$$

For $h = 0$ and $P = 0$ it is

$$\ddot{x} - x + x(x^2 + y^2) = 0 \qquad \ddot{y} - y + y(x^2 + y^2) = 0. \tag{3}$$

This is the model of non-linear conservative rotor system. The static equilibrium positions are

$$\begin{array}{lll} \text{for } x = 0: & y = \pm 1 & \text{for } y = 0: \quad x = \pm 1 \\ & y = 0 & \qquad\quad x = 0. \end{array}$$

Analysing the stability of positions it is

$$\left.\begin{array}{ll} x = 0 & y = \pm 1 \\ y = 0 & x = \pm 1 \end{array}\right\} \quad \text{stable positions}$$

$$x = 0 \qquad y = 0 \qquad \text{unstable position.}$$

By multipying the first equation in system (3) by $\dot{x}$ and the second by $\dot{y}$ the summarized equation is

$$(\dot{x}\ddot{x} + \dot{y}\ddot{y}) - (x\dot{x} + y\dot{y})(x\dot{x} + y\dot{y})(x^2 + y^2) = 0. \tag{4}$$

After integration it is

$$(1/2)(\dot{x}^2 + \dot{y}^2) - (1/2)(x^2 + y^2) + (1/4)(x^2 + y^2)^2 = C \tag{5}$$

where

$$\cdot\ T = (1/2)(\dot{x}^2 + \dot{y}^2) \quad \text{— kinetic energy} \tag{6}$$

$$V = (1/4)(x^2 + y^2)^2 - (1/2)(x^2 + y^2) \quad \text{— potential energy.} \tag{7}$$

The equation (5) represents the statement that the sum of kinetic and potential energy is constant and it is expected in a conservative system. The value of constant C is a function of initial conditions. The property of motion depends on the value of the constant.

In Fig. 5 the potential energy (7) in function of amplitude A or deflection coordinates x and y of the rotor's center and the phase portraits are plotted. The vibration response is

$$A = (x^2 + y^2)^{1/2}. \tag{8}$$

If the initial conditions are such to give $C = C_0$ there are two centers C_1 and C_2 (Fig. 5.a) in $x = \pm 1$ and $y = \pm 1$. For $C = C_3$ there are two curves which intersect in the point $x = \dot{x} = 0$ and $y = \dot{y} = 0$ (Fig. 5.b). This is a separatrix curve with saddle point. If $C_0 < C < C_3$ there are two curves around the centers C_1 and C_2. This is the "small orbit" (Fig. 5.c). For $C > C_3$ there is only one curve surrounding all the three equilibria. That is the "large orbit" (Fig. 5.d).

So, there exist two types of periodic steady-state oscillations: local osscilations with small orbit and global oscillations with large orbit.

Now, let damping be introduced:

$$\begin{aligned} \ddot{x} + h\dot{x} - x + x(x^2 + y^2) &= 0 \\ \ddot{y} + h\dot{y} - y + y(x^2 + y^2) &= 0. \end{aligned} \tag{9}$$

The system is no more conservative and an integrated energy expression is no longer possible. However, one can still perturb the equation about its equilibria and conclude about the motion in phase-plane. The rotor's center moves towards

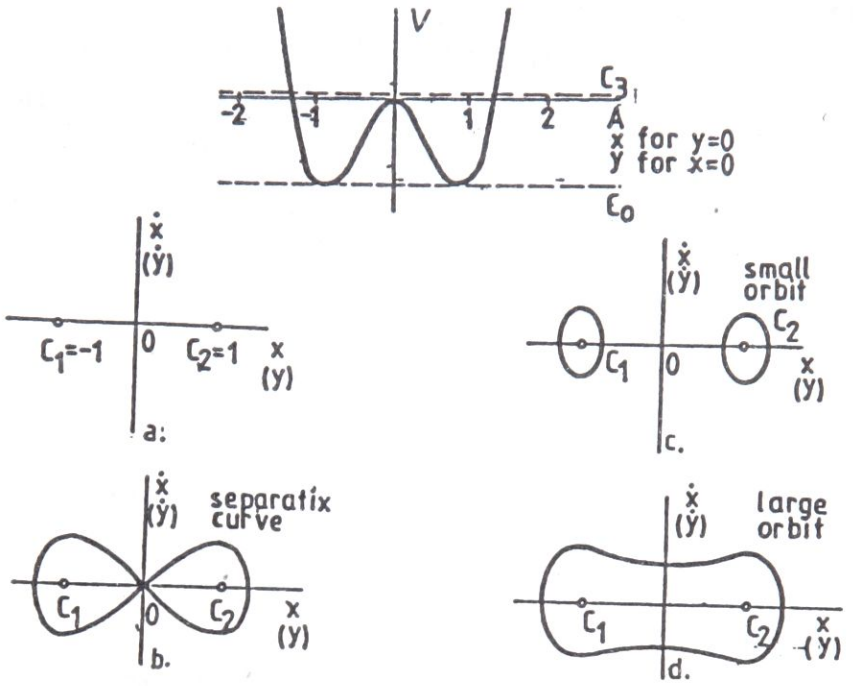

Fig. 5. Potential energy shema and phase portraits of: a) centers, b) separatrix curve, c) small orbit, d) large orbit.

the points with minimal potential energy. These are stable focuses C_1 and C_2. The rotor rotates around the stable position.

The chaotic motion is produced by the forcing funkction. The system described by (1) has some periodic oscillations with small orbit or large orbit, while the amplitude P and frequency Ω of excitation force does not exceed a certain critical value. Then, on increasing parameter Ω large orbit motion would jump into small orbit oscillations — the jump phenomena belongs to the most characteristic features of nonlinear vibrating systems. Jump phenomena of this type does not occur in that case. Instead, when exceeds a critical value, large orbit turns into an irregular motion consisting essentially on random like jumps from oscillations around $x = -1$ or $y = -1$ and back. The motion does not decay and in a long time interval shows properties of a "steady-state" behaviour (Fig. 3.c).

In Fig. 6 the time history is shown from large orbit oscillation, chaotic motion to small orbit oscillation.

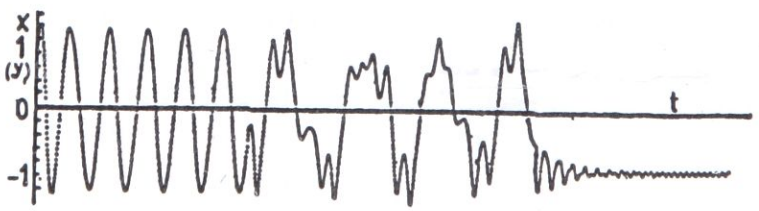

Fig. 6. Time history for various excitation frequences

7. Analytical Method for Denoting Chaos. An analytical criterion for chaos is given. It is based on the stability of the approximate analytical T-periodic solution. Such analytical methods are developed for Duffing oscillators with soft and hard properties, negative and zero characteristics which are general for all types of Duffing equations. The approximative solution to (1) is considered

$$z = Ae^{i(\Omega t+\theta)}. \tag{10}$$

The constant values of the amplitude A and the phase θ of the oscillation are determined by applying the balance method of the leading first harmonic.

By substituting (10) into (1) and separating the real and imaginary parts the following relations are obtained

$$\text{Re:} \quad -A\Omega^2 - A + A^3 = P\cos\theta, \qquad \text{Im:} \quad hA\Omega = -P\sin\theta. \tag{11}$$

The amplitude-frequency resonant curve is derived by eliminating θ

$$A^2\left(h^2\Omega^2 + (A^2 - \Omega^2 - 1)^2\right) = P^2. \tag{12}$$

These resonance curves for various values of amplitude of the exciting force is plotted in Fig. 7. For small values of P the resonance curve consistes of two parts. These two parts approach each other as P is increased. The corresponding critical value of P_{cr} is

$$P_{cr} = 2\sqrt{3}/9. \tag{13}$$

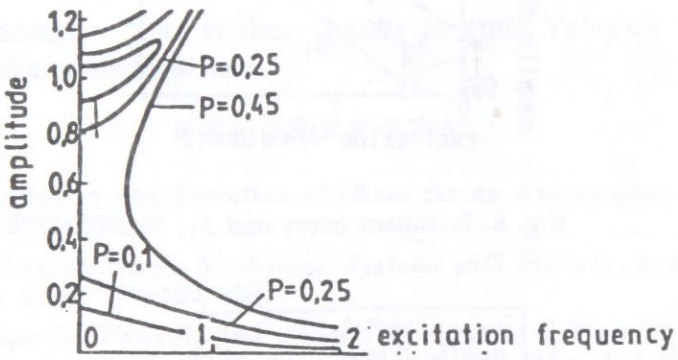

Fig. 7. Amplitude-frequency properties for various values of excitation force

The stability of the solution (10) is studied by means of the method of varying amplitudes and phase angles. Let the perturbed solution be represented as

$$z = (A + u)e^{i(\Omega t+\theta+v)} \tag{14}$$

with small perturbations u and v which depend on t. Let us substitute the relation (14) into (1) and retain only linear terms in the perturbations u and v and take into account the amplitude-frequency relation (12). This results in the following system of two linear differential equations with constant coefficients

$$\begin{aligned} &\ddot{u} + h\dot{u} + u(-\Omega^2 - 1 + 3A^2) - 2\dot{v}A\Omega - hvA\Omega = 0 \\ &\ddot{v}A + h\dot{v}A + v(-A + A^3 - A\Omega^2) + 2\dot{u}\Omega + hu\Omega = 0. \end{aligned} \tag{15}$$

The solutions of equations are: $u = Ue^{\rho t}$, $v = Ve^{\rho t}$.

$$\begin{aligned} &\rho^2 U + h\rho U + (-\Omega^1 - 1 + 3A^2) - 2\rho V A\Omega - hVA\Omega = 0 \\ &\Omega^2 VA + hV\rho A + V(-A + A^3 - A\Omega^2) + 2U\rho\Omega + hU\rho = 0. \end{aligned} \tag{16}$$

The characteristic equation is

$$b_0\rho^2 + b_1\rho + b_2 = 0 \tag{17}$$

where

$$b_0 = h^2 + 4\Omega^2 \tag{18}$$

$$b_1 = 2h(-1 + \Omega^2 + 2A^2) \tag{19}$$

$$b_2 = h^2\Omega^2 + (-\Omega^2 - 1 + 3A^2)(-\Omega^2 - 1 + A^2). \tag{20}$$

The form of the eq. (17) is the same as for the one-degree-freedom system with soft characteristic [22].

For positive damping ($h > 0$) the conditions of stability are

$$-1 + \Omega^2 + 2A^2 > 0 \qquad (S_2 \text{ curve}) \tag{21}$$

$$h^2\Omega^2 + (-\Omega^2 - 1 + 3A^2)(-\Omega^2 - 1 + A^2) > 0 \qquad (S_1 \text{ curve}). \tag{22}$$

The resonant curve and the boundary curves S_1 and S_2 are shown in Fig. 8 for $h = 0.2$ and $P = 0.25$.

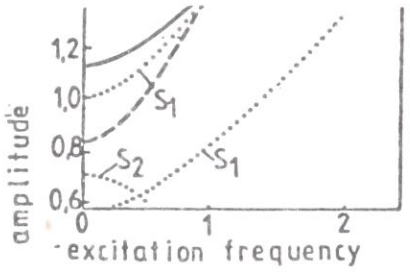

Fig. 8. Resonant curve and S_1, S_2 curves.

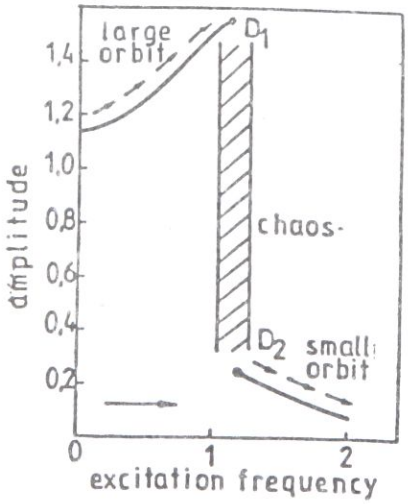

Fig. 9. The region of energy dissipation (hysteresis type behaviour).

Stable parts of resonant curve are represented by full lines and the unstable parts by dashed lines.

A transitation from stability to instability is found to occur at the frequency $\Omega = 1.0$ where the curve S_1 interrsects the upper branch.

8. Comparation of Numerical and Analytical Solutions. Analysing the results got in the chapter 4 and 7 it can be concluded that the analytical method gives the result which is in vicinity with numerical results. In the neighbourhood of the value $\Omega = 1.0$ (which is got analytically) is the region where bifurcation occur and chaotic motion appears (Fig.9). In that region dissipation occurs.

9. Conclusion. The motion of the strong non-linear and excited rotor varies by varying the parameters of excitation and the initial conditions.

In the paper the influence of excitation frequency on the motion is analysed. For observation of motion as descriptors the portraits in $x - y$, $x - \dot{x}$, $y - \dot{y}$ plane, the portrait in Poincare map and time history diagrams $(x - t, y - t, A - t)$ are applied. The mathematical model of the rotor is a system of non-linear and non-homogenous differential equations. For numerical integration the Runge-Kutta method is applied. By increasing of excitations frequences the motion varies from a limit cycle motion to chaotic motion. It is proved by Feigenbaum universal constant. An analytical method for denoting of the chaotic motion is developed based on the well known analytical methods for the one-degree-freedom systems. The obtained value is in vicinity of the value at which chaotic behaviour of rotor's center begins.

Acknowledgments. The author thanks to Ass. Valentin Glavardanov for his contribution in this investigations.

REFERENCES

[1] Dowell E. H.: *Observation and Evolution of Chaos for an Autonomous System*, JAM, Vol. **51**, No. 3, pp. 664–674, 1984.

[2] Awrercewicz J.: *Chaos in Simple Mechanical Systems with Friction*, J. of Sound and Vibration, Vol. **109**, No. 1, pp. 178–180, 1986.

[3] Bapat C. N., Sankar S.: *Periodic and Chaotic Motions of a Mass Spring System Under Harmonic Force*, J. of Sound and Vibration, Vol. **108**, No. 3, pp. 533–536, 1986.

[4] Steeb W. H., Kunick A.: *Chaos in Limit Cycle Systems with External Periodic Excitations*, Int. J. of Nonlinear Mechanics, Vol. **22**, No. 5, pp. 349–361, 1987.

[5] Fang T., Dowell E. H.: *Numerical Simulation of Periodic and Chaotic Response in a Stabler Duffing System*, Int. J. of Nonlinear Mechanics, Vol. **22**, No. 5, pp. 401–425, 1987.

[6] Tongue B. H.: *Characteristics of Numerical Simulations of Chaotic Systems*, JAM, Vol. **54**, No. 3, pp. 695–700, 1987.

[7] Holmes P. J., Moon F. C.: *Strange Attractor and Chaos in Nonlinear Mechanics*, JAM, Vol. **50**, No. 4, pp. 1021–1023, 1983.

[8] Tongue B. H.: *Existence of Chaos in a One-Degree-Freedom System*, J. of Sound and Vibration, Vol. **110**, No. 1, pp. 69–78, 1986.

[9] Rudowski J., Szemplinska-Stupnicka W.: *On a Approximate Criterion for Chaotic Motion in a Model of a Buckled Beam*, Ing. Archiv, Vol. **57**, pp. 243–255, 1987.

[10] Dowell E. H., Pezeshki O.: *On the Understanding of Chaos in Duffing Equations Including a Comparation with Experiment*, JAM, Vol. **53**, No. 1, pp. 5–10, 1986.

[11] Thompson J. M. T., Stewart H. B.: *Nonlinear Dynamics and Chaos*, John Wiley and Sons, New York, pp. 376, 1988.

[12] Guckenheimer J., Holmes P.: *Nonlinear Oscillations, Dynamical Systems and Bifurcations of Vector Fields*, Springer Verlag, New York, pp. 459, 1987.

[13] Muszynska A.: *On Rotor Dynamics*, PAN, Warsaw, 1976.

[14] Szopa J., Bestle D.: *On the Application of Stochastic Sensitivity Functions to Chaotic Systems*, J. of Sound and Vibration, Vol. **104**, No. 1, pp. 176–178, 1986.

[15] Kapitaniak T.: *Quantifying Chaos with Amplitude Probability Density Function*, J. of Sound and Vibration, Vol. **114**, No. 3, pp. 588–592, 1987.

[16] Kapitaniak T.: *Combined Bifurcations and Transition to Chaos in a Non-Linear Oscillator with Two External Periodic Forces*, J. of Sound and Vibration, Vol. **121**, No. 2, pp. 259–268, 1988.

[17] Kapitaniak T.: *Chaos in a Noisy Mechanical System with Stress Relaxation*, J. of Sound and vibration, Vol. **123**, No. 3, pp. 391–396, 1988.

[18] Bert C. W., Stricklin J. D.: *Comparative Evalution of Six Different Numerical Integration Methods for Non-Linear Dynamic Systems*, J. of Sound and Vibration, Vol. **127**, No. 2, pp. 221–229, 1988.

[19] Szemplinska-Stupnicka W.: *Bifurcations of Harmonic Solution Leading to Chaotic Motion in the Softening Type Duffing Oscillator*, Int. J. of Nonlinear Mechanics, Vol. **23**, No. 4, pp. 257–279, 1988.

[20] Szemplinska-Stupnicka W., Bajkowski J.: *The 1/2 Subharmonic Resonance and its Transition to Chaotic Motion in a Nonlinear Oscillator*, Int. J. of Nonlinear Mechanics, Vol. **21**, No. 5, pp. 401–419, 1986.

[21] Szemplinska W.: *Secondary Resonances and Approximate Models of Routes to Chaotic Motion in Nonlinear Oscillator*, J. of Sound and Vibration, Vol. **113**, No. 1, pp. 155–172, 1987.

[22] Dooren R.: *On the transition from Regular to Chaotic Behaviour in the Duffing Oscillator*, J. of Sound and Vibration, Vol. **123**, No. 2, pp. 327–339, 1988.

DIE CHAOTISCHE BEWEGUNG DES ROTORS

In dieser Arbeit ist die Bewegung des Rotorzentrums bei der Änderung der Anregungsfrequenz analysiert worden. Das Rotormodell ist ein nichtlineares Welle-Diskus-System. Die numerische Schreiber der Bewegung sind die Porträte in den $x-\dot{x}$, $y-\dot{y}$, $x-y$ Ebenen, die Zeitdiagramme $x-t$, $y-t$, $A-t$ und die Poincare Mappe. Die Frequenzanhebung ändert den Bewegungscharakter: von üblicher rückweiser Bewegung auf der grossen Bahn über der chaotischen Bewegung bis zur üblichen rückweisen Bewegung auf der kleinen Bahn. Die chaotische Bewegung ist die Wirkung der ausseren Zwangskraft auf dem nichtlinearen Rotor.

HAOTIČNO KRETANJE ROTORA

U radu je numerički analizirano kretanje središta rotora pri promeni frekvencije pobude. Model rotora je nelinearan vratilo-disk sistem. Numerički opisivači kretanja su portreti u $x-\dot{x}$, $y-\dot{y}$, $x-y$ ravnima, vremenski dijagrami $x-t$, $y-t$, $A-t$ i Poincare mapa. Porastom pobudne frekvencije menja se karakter kretanja od ustaljenog periodičnog kretanja po velikoj orbiti do ustaljenog periodičnog kretanja po maloj orbiti. Haotično kretanje je rezultat dejstva spoljašnje prinudne sile na nelinearan rotor koja početnim uslovima unosi određenu energiju u sistem koji je osetljiv na promenu energetskog nivoa sistema čime se generišu kretanja različitog karaktera. U radu je dat i analitički kriterijum vrednosti frekvencije pri kojoj dolazi do pojave haotičnog kretanja.

Dr Livija Cvetićanin,
Fakultet tehničkih nauka,
V. Vlahovića 3
21000 Novi Sad